

Statistical analysis and automation through machine learning of resonant ultrasound spectroscopy data from tests performed on complex additively manufactured parts

Anne-Françoise Obaton (✉ anne-francoise.obaton@lne.fr)

Laboratoire National de Métrologie et d'Essais

Nasim Fallahi

Engineering Ingegneria Informatica

Anis Tanich

Laboratoire National de Métrologie et d'Essais

Louis-Ferdinand Lafon

Laboratoire National de Métrologie et d'Essais

Gregory Weaver



Weaver NDT

Research Article

Keywords: Additive Manufacturing (AM), Resonant Ultrasound Spectroscopy (RUS), statistical analysis, Machine Learning (ML), Un-supervised K-means, Neural network

Posted Date: October 28th, 2022

DOI: <https://doi.org/10.21203/rs.3.rs-2166993/v1>

License:   This work is licensed under a Creative Commons Attribution 4.0 International License. [Read Full License](#)

Additional Declarations: No competing interests reported.

Version of Record: A version of this preprint was published at Journal of Nondestructive Evaluation on January 24th, 2024. See the published version at <https://doi.org/10.1007/s10921-023-01035-8>.

Abstract

Additive manufacturing brings inspection issues for quality assurance of final parts because non-destructive testing methods are faced with shape complexity, size, and high surface roughness. Thus, to drive additive manufacturing forward, advanced non-destructive testing methods are required. Methods based on resonant ultrasound spectroscopy (RUS) can take on all the challenges that come with additive manufacturing. Indeed, these full body inspection methods are adapted to shape complexity, to nearly any size, and to high degrees of surface roughness. Furthermore, they are easy to implement, fast and low cost. In this paper, we present the benefit of a resonant ultrasound spectroscopy method, combined with a statistical analysis through Z score implementation, to classify supposedly identical parts, from a batch. We also demonstrate that the inspection can be further accelerated and automated, to make the analysis operator independent, whether the analysis of the resonant ultrasound spectroscopy data is performed supervised or unsupervised with machine learning algorithms.

Introduction

To be able to rely on the integrity of parts additively manufactured (AM), their inspection is required prior to use. However, one of the main benefits of AM is to build very complex part geometries, such as cavities, internal channels, free forms, lattices, which do not facilitate ease of inspection. Besides being non-destructive, the quality method needs to be volumetric, and capable of complex shapes and rough surfaces. The challenge is high. X-ray computed tomography (XCT) meets these requirements, but is strongly limited by the size and density of the parts. Among other investigated methods on complex AM parts, resonant ultrasound spectroscopy (RUS) methods have shown particularly promising [1, 2]. The principle of these full body methods is based on the analysis of the positions, in frequency, of the resonant vibrational modes of the part under test as a result of an impulse excitation. Shifts in frequency of the positions of the resonant peaks compared to parts from the same family or simulations is synonymous of a difference in the integrity of the part. These full body methods have the advantage of being faster, easier to use, and cheaper than XCT, but also suitable for large and dense parts. Additionally, by implementing machine learning (ML) algorithms on the collected RUS data for clustering or classification, using unsupervised and supervised algorithms respectively, the data analysis can be automated. Indeed, ML algorithms can provide significant advantages for the automation of non-destructive evaluation (NDE) and test (NDT) in different condition monitoring applications for various materials and structures [3]. Harley and Sparkman, in 2019, showed that the use of ML to solve NDE problems could provide a potential revolution for future NDE challenges [4].

Typically, RUS enables the detection of parts as acceptable or unacceptable from a training set of known parts. We have already demonstrated the capability of RUS on a set of parts without any (acceptable parts) and with known internal features simulating typical AM defects, designed in the numerical model, on dense stainless steel AM parts containing different numbers of internal features [1, 2]. In this specific case, we have shown that RUS allowed the separation of the acceptable and unacceptable dense parts but could not sort the parts according to the number of features they contained. However, on cobalt-chromium AM lattice structures with various numbers of missing struts, not only the analysis of the RUS data enabled separating the parts with and without missing struts, but also nearly the entire set of parts, could be classified according to the number of missing struts [3].

In addition, RUS enables the classification of different sets of parts according to their manufactured process parameters. We have already demonstrated this capability of RUS on a set of parts additively manufactured with various machine parameters (wall thicknesses, laser powers, scanning speeds, and scanning strategies) [5]. The RUS data statistical analysis allowed the classification of all parts according to their process parameters.

In this paper, we propose to present the statistical analysis, through Z-scores implementation, of the RUS data of a batch of parts supposedly identical and to automate the whole analysis by implementing ML algorithms as a post-processing model to make the analysis operator independent: 1) considering only the available RUS data, an unsupervised model was implemented. Then based on the clustering performed by the unsupervised model, a supervised model was initiated; 2) the available RUS data were considered as well as the results of the Z-score analysis to identify acceptable and unacceptable parts for labelling the data and generating virtual parts. Considering these data, several supervised models were implemented.

This article is structured as follows. Section 2 describes the basic principle of RUS methods in general, and then focuses on the specificities of impulse excitation methods (IEM), a type of RUS. Section 3 presents the AM parts which were investigated in this study and section 4, their NDT with an IEM. Sections 5 and 6 address, respectively, the Z-score and ML IEM data analysis of the investigated parts. Finally, section 6 draws conclusion.

1. Principle Of The Experimental Method

In this study, a Resonant Ultrasound Spectroscopy (RUS) method was used to identify each part's conformity in regard to its group of like parts. RUS takes advantage of the correlation between the resonance properties of the mechanical vibration modes of a part and its intrinsic properties, such as its geometry, density, elasticity, and internal and external structure, to detect defects and material variations in the part. The basic principle of this whole body non-destructive examination technique is to excite and record, in the acoustic and/or ultrasonic ranges, the spectrum of the natural resonant frequencies of the vibration modes of the part and to compare it to the spectra of an established acceptable resonant frequency pattern (reference parts or parts from the same group or simulations). Any shift in resonant frequency between the spectrum of the part under test and the spectra of the pattern will be the signature of a difference between the part and the pattern. Thus, the method enables classification of the parts as acceptable or unacceptable or according to their intrinsic properties.

According to ASTM E2001 [] standard, RUS includes two types of methods: swept sine or impulse excitation methods (IEM). We will focus on IEM as an IEM type of method was used in the frame of this study. In IEM (Fig. 1), the part is excited with a mechanical impact (hammer) to stimulate its natural resonant frequencies, then its vibration response is captured with a measurement transducer (microphone, piezo transducer, accelerometer, laser vibrometer), recorded, processed, and analyzed with a data acquisition device and software. In the present study, the IEM system was comprised of hardware including a modal instrumented hammer to induce vibration to the part, a microphone to collect the part response, a high-speed analog to digital converter (24 bits) to perform a Fast Fourier Transform (FFT) that provides frequency spectra. Finally, a software program is enabled to display the spectra and to define frequency ranges of acceptable variability around the established resonant frequency pattern peaks to sort the parts. This simple principle makes IEM particularly easy and fast to implement.

2. Description Of The Tested Parts

The investigated parts (Fig. 2) were manufactured in the titanium alloy TA6V ELI (Ti-6Al-4V), by Safran, using a laser powder bed fusion (PBF-LB) machine, Renishaw 500Q, Y48 implementing 3 lasers.

In total, a group of 27 like parts were manufactured but only 24 were provided for RUS examination. The parts are labelled from 1 to 27 (parts 15, 16, and 21 were not provided). They were manufactured on three different platforms (Fig. 2a): parts 1 to 9 on platform 1, parts 10 to 18 on platform 2, and parts 19 to 27 on platform 3. After manufacturing, the part went through the following post-treatment: 1) powder removal, 2) first sandblasting, 3) second

sandblasting, 4) heat treatment to release residual stress, 5) support removal, 6) visual inspection, and 7) hot isostatic pressing (HIP).

3. Experimental Examination Of The Tested Parts

For repeatability, thirty tests were performed on each part, positioned on foam, and impacted at approximately the same location. The influence of the impact's location was examined prior to the tests and was considered to be negligible. The acquisitions were performed in the range of 0–94 kHz with a resolution of 1.465 Hz corresponding to an acquisition time of 0.683 s. The first thirteen resonant peaks, located in the range of 0–20 kHz (Fig. 3), turned out to contain all the required information to classify the parts. Thus, in the following statistical analyses, only this range of the spectra was considered.

4. Z-score Analysis Of The Tested Parts

The objective of this analysis is to classify the parts into various risk categories computing Z-score statistical tool which, beyond its simplicity of execution, offers a physical interpretation. A Z-score is used to compare a sample's location within a population of reference samples. It expresses the deviation of the sample from the mean value of the reference samples' population in terms of standard deviation on the population taken as reference. For this study, any sample lying in between [-1, 1] Z-score is acceptable to the population, if it is between [-2, -1]U[1, 2] it is considered as low risk, if it is between [-2.5, -2]U[2, 2.5] it is considered as medium risk and outside these intervals as high risk. These are arbitrary grouping choices based on statistical separation.

The Z-scores were computed with the frequencies at maximum amplitude of the first thirteen peaks (< 20 kHz) using this relation:

$$Z_{score} = \frac{\text{peak frequency of a sample} - \text{mean of the peak frequencies of reference samples' population}}{\text{standard deviation of the peak frequencies of the reference samples' population}}$$

1

Before undertaking the main statistical analysis to compare all the parts to each other independently of their original platform, the bias between the three platforms was examined to ensure that there was no platform effect. To do this, the Z-scores on the frequency resonant peaks, for each of the series of parts manufactured on the same platform, were computed considering first all the parts on each platform as reference (Fig. 4) and then considering the average of the parts of the three platforms as reference (Fig. 5).

From Fig. 4, it can be observed that all Z-scores, for all platforms, whatever the chosen reference, are concentrated in the interval [-2, 2] except for three parts: S18 from platform 2, S20, and S24 from platform 3. A similar phenomenon was observed when considering all platforms as reference (Fig. 5). In this case, all parts are concentrated in the interval [-1, 1] except the three previously listed parts as well as S8 from platform 1. These four parts were not manufactured on the same platform so one can conclude that it is a part effect and that the platform effect is negligible. Thus, the parts do not need to be linked to their manufacturing platform in the main analysis.

As all the parts are supposed to be identical, in order to select reference parts for the Z-score analysis, first, all parts, from all platforms, were considered as reference. This step enables identification of the parts located in the interval [-1, 1] to be chosen as reference parts for the final Z-score analysis plotted in Fig. 6.

As observed in Fig. 6, most of the parts are located in the interval [-1, 1]. This means that these parts respond similarly across all the frequencies and that they should be similar in material properties and dimensions. However, there are five

outliers: S8 (platform 1), S13 and S18 (platform 2), S20 and S24 (platform 3). S24 is the weakest part in the batch as the frequencies of its resonant peaks are shifted to lower frequencies (Fig. 7). Generally, lower frequencies are driven by a defect or low mechanical properties. S20 (Fig. 7) and S13 are in the same situation to a lesser degree. The deviation from S8 and particularly S18 could be rather attributed to grain size, stress, or dimensional variations as the shift of their resonant peaks goes toward higher frequencies []. These outliers were not manufactured at the same location on their respective platform so their difference cannot be linked to that cause. Only S24 is outside the interval [-2, 2], thus, for the ML analysis, S24 is the only outlier noted.

5. Machine Learning Analysis Of The Tested Parts

Machine learning (ML), on the RUS data, was computed for the purpose of automating the whole analysis, to make the RUS analysis operator-independent.

ML is divided into two categories: unsupervised and supervised. The use of one or the other depends on the initial available data []. In supervised learning, a set of data for which to each input corresponds an output (the data are said to be labelled or targeted) must be available to predict the output of new data. Whereas, in unsupervised learning, the analysis is based on un-labelled data that are simply grouped together for a better view and understanding of them. In both cases, models are trained to predict classes (supervised) or clusters (unsupervised) of the data. Then to evaluate which model is the more performing, each of them is compared to each other in terms of accuracy and sensitivity of the model to evaluate the number of false negatives that would correspond to a defective part reported as compliant.

In this paper, first, considering only the available RUS data, an unsupervised model was implemented on the frequencies at the maximum amplitude of the first thirteen peaks (< 20 kHz). Then based on the clustering performed by the unsupervised model, a supervised model was run; Second, the available RUS data were considered as well as the results of the Z-score analysis to identify acceptable and unacceptable parts for labelling the data and generating virtual parts. Considering these real and virtual data, several supervised models were implemented on the frequencies at maximum amplitude of the first thirteen peaks (< 20 kHz) as well as on the whole spectra up to 20 kHz.

5.1 Automated unsupervised followed by supervised analysis to label parts

5.1.1 Unsupervised analysis

An unsupervised K-means analysis [], a data clustering, and recognition method enabling to distinguish data similarity and dissimilarity was implemented. In this study, four clusters, using the Euclidian distance, were used to categorize the data with peaks as input (first 13 peaks at maximum frequency in the range < 20 kHz). In Fig. 8, the four clusters are shown in different colors and their center are indicated. As it shown, cluster number four is including two samples which are S20 and S24, outliers in the Z-score analysis. The output results of the unsupervised method are used for evaluation and accuracy level in neural network supervised methods in the next section.

5.1.2 Supervised analysis

A Neural Network (NN) model [] was used to link the input and output data with a series of interconnected neurons. The method consists of three steps: training, validation, and testing. The training phase involves determining the relationship between input and output data []. The data splitting is random, the training algorithm is based on Levenberg-Marquardt and the performance is firmed by Mean Squared Error (MSE) with ten layers []. The performance

for the current problem is based on MSE on the validation set with respect to the number of iterations in Levenberg-Marquardt. The model's optimal performance was 0.6180 at the 6th iteration.

The MSE and coefficient of determination (R^2) are two statistical metrics that are commonly used to assess and validate the model's reliability. The results are displayed for three subsets in Table 1: training, validation, and testing, based on the correlation between the expected outputs and predictions. The closer the R^2 is to 1, the better the fit and model.

Table 1
Training, validation and test results through NN

	Data splitting (%)	MSE	R
Training	70	0	1.0000
Validation	15	0.6180	0.9648
Test	15	0.0994	0.9307

In summary, we have shown that the K-means clustering method and the NN supervised algorithm can be implemented as post-processing classification methods to automate the RUS data analysis.

5 – 2 Supervised analysis based on Z-score results to label parts

To implement the supervised analysis, the RUS data on the 24 real parts were considered and, to increase the amount of data, 9 virtual outliers and 68 inliers were generated in order to have a total of 100 parts to run the models. A rate of 10% was taken for outliers to be as representative as possible of industrial cases. The virtual outliers were generated in a random and uniform manner. Some of their peaks were shifted toward lower or higher frequencies based on the frequency shifts observed for all real part spectra compared to the mean reference part spectra. The virtual inliers were generated by concatenation of the twenty three spectra of the real inliers parts according to the Z-scores results. Then, to perform the analysis, the whole set of parts was distributed into three groups: 70% of the parts were considered for training, 15% for validation and 15% for testing. First, the training set was used to find the models parameters. Second, the validation set was injected in all models to find the best combination of model and hyper-parameters. Finally, the test set enabled to evaluate the capacity of prediction of the best model on new data. For a better estimation of the capacity of prediction, a stratified cross-validation was performed: different train and validation sets were selected in a loop (70% train and 15% validation) and the capacity of prediction was computed at each iteration. 15% of the data was kept for testing the model at the end of the cross-validation.

The supervised analysis was performed in parallel for comparison: 1) on the frequencies at the maximum amplitude of the first thirteen resonant peaks (< 20 kHz); 2) on the whole spectra up to 20 kHz. Prior to analysis, noise reduction was applied on the spectra [1]: 1) a baseline correction was applied on the spectra, 2) if the amplitudes were positives, they were kept as they are and, if they were negatives, they were set to zero. For the ML analysis, several supervised algorithms had been executed but only the four showing the highest accuracy were selected at first: 1) SVM (Vector Machine Support) with four different "kernel" hyper-parameters (radial, polynomial, sigmoid, and linear), 2) the K-NN model (K Nearest Neighbours) with the hyper-parameter k taking three different values (k = 5, k = 10 and k = 15) then two models without hyper-parameter modifications: 3) the Naïve Bayes model and 4) the decision tree [2]. Second, the

three most efficient combinations “model and hyper-parameter” were selected to go further: 1) SVM with the radial kernel, 2) SVM with polynomial kernel and 3) Naïve Bayes.

The mean and the standard deviation (Std) on the accuracy, as well as the mean and Std on the sensitivity are given in Table 2 for the frequencies at the maximum amplitude of the first thirteen resonant peaks (< 20 kHz). These metrics were calculated by stratified cross-validation on the validation sets.

Table 2
Performance prediction of ML models, on the validation sets, with peaks as input

Model	mean accuracy	accuracy std	mean sensitivity	sensitivity std
SVM polynomial kernel	0.89	0.04	0.20	0.27
SVM radial kernel	0.91	0.06	0.30	0.44
Naïve Bayes	0.89	0.24	1.00	0.00

From Table 2, one can be observed, that during the validation, the three mean accuracies are close to each model. To differentiate them, one can compare their mean sensitivity which represents the rate of unacceptable parts compared to acceptable parts. From this point of view, the Naïve Bayes model stands out. A 5-fold cross-validation, on the validation sets, was performed, from which five confusion matrices were extracted. In the best cases, the confusion matrices were the same for both models. However, in the worst cases, the Naive Bayes model has a false negative rate of 0% and a high false positive rate which is positive whereas it is the opposite for the SVM kernel radial model. As the best compromise between high accuracy and sensitivity is required, the Naïve Bayes model was selected and evaluated on the test set (Fig. 9). Its performance reached an accuracy and sensitivity of 100%. Therefore, the Naïve Bayes model is a good candidate for the analysis of the resonance peaks.

The mean precision, mean sensitivity, standard deviation on precision and of sensitivity, also calculated by stratified cross-validation on the validation sets, are given in Table 3 for the whole spectra up to 20 kHz.

Table 3
Performance prediction of ML models, on the validation sets, with spectra as input

Model	mean accuracy	accuracy std	mean sensitivity	sensitivity std
SVM polynomial kernel	0.85	0.03	0.00	0.00
SVM radial kernel	0.88	0.10	0.30	0.45
Naïve Bayes	0.92	0.06	0.53	0.36

Considering the analysis with the spectra as input, Table 3 shows that the Naïve Bayes model has the highest mean sensitivity and a mean accuracy above 90%. This model is therefore also the best candidate when considering all the data provided by the spectra instead of only the frequencies at maximum amplitude. However, the mean sensitivity of 53% is much lower in the present case. Five confusion matrices were calculated with five different combinations of the selected 15% validation sets as before. The confusion matrix for the Naïve Bayes model, on the test set, is presented in Fig. 10 left. The confusion matrices on validation sets, for peaks and spectra as input, are the same. However, the confusion matrices for the test set with spectra as input displays 6.7% of false negative. Furthermore, considering that the mean sensitivity is only 53% compared to 100% for the peaks (Table 1), one can conclude that the Naïve Bayes is more effective for peaks than for spectra as input.

In order to confirm that the Naïve Bayes model works properly, it was tested with the twenty-four real labelled parts. The results are displayed in Fig. 10 right. The matrix indicates that 1 parts over the 24 was not predicted correctly. It was predicted false positive i.e. unacceptable instead of acceptable. Otherwise, the rest of the parts was predicted correctly, 22 parts are acceptable and 1 parts over 24 is non-acceptable.

In summary, among the three ML models which were investigated, one of them stand out for its high mean accuracy and sensitivity: the probabilistic Naïve Bayes model. However, the mean sensitivity is not high when considering spectra as input rather than peaks. Moreover, the model applied on the spectra is more time-consuming. Thus, the ML Naïve Bayes model should be implemented on peaks rather than on spectra to automate the RUS data analysis.

6. Conclusion

The adoption of AM in the industry is going slowly because the qualification of parts is an issue regarding their possible complexity in geometry, their size and their high surface roughness. In addition to being adapted to complex geometries, nearly any size, and high roughness, the evaluation must be non-destructive, and ideally simple to implement, fast, and inexpensive. These require innovation in the NDT sector. The RUS method described here, combined with Z-score analysis and/or ML, is a solution from these perspectives. The method is suitable for any shape, size, and surface roughness. It is also easy to implement, fast and inexpensive. And combined with Z-score analysis and/or ML, it enables to be fully automated and thus expedites the part qualification process, which lowers the costs of validation quality control.

In the current paper, we have presented an application of RUS through IEM and addressed statistical methods such as Z-score, supervised and unsupervised models to automate successfully the analysis of RUS data on a batch of supposedly identical parts.

Declarations

***Ethics approval and consent to participate**

Not applicable.

***Consent for publication**

The authors give consent for publication.

***Availability of data and material**

All of the data and material are owned by the authors and/or no permissions are required.

***Competing interests**

I declare that the authors have no competing interests as defined by Springer, or other interests that might be perceived to influence the results and/or discussion reported in this paper.

***Funding**

Not applicable.

***Authors' contributions**

Anne-Françoise Obaton wrote the main manuscript text and performed the RUS experiments (section 3).

Gregory Weaver and Anis Tanich performed the Z-score analysis (section 4).

Nasim Fallahi performed the automated unsupervised followed by supervised analysis to label parts (section 5.1).

Anis Tanich and Louis-Ferdinand performed the supervised analysis based on Z-score results to label parts (section 5.2).

All authors reviewed the manuscript.

***Acknowledgements**

Not applicable.

References

1. Obaton A-F, Butsch B, McDonough S, Carcreff E, Laroche N, Gaillard Y, Tarr J, Bouvet P, Cruz R, Donmez A (2020) Evaluation of Nondestructive Volumetric Testing Methods for Additively Manufactured Parts. In Structural Integrity of Additive Manufactured Parts, N. Shamsaei, S. Daniewicz, N. Hrabe, S. Beretta, J. Waller, and M. Seifi: West Conshohocken, PA, pp 51–91, <https://www.astm.org/stp162020180099.html>
2. Obaton A-F, Butsch B, Carcreff E, Laroche N, Tarr J, Donmez A (2020) Efficient Volumetric Non-Destructive Testing Methods for Additively Manufactured Parts. *Weld World* 64:8:1417–1425. <https://doi.org/10.1007/s40194-020-00932-0>
3. Obaton AF, Wang Y, Butsch B, Huang Q.A (2021) Non-Destructive Resonant Acoustic Testing and Defect Classification of Additively Manufactured Lattice Structures *Weld World* 65:361–371. <https://doi.org/10.1007/s40194-020-01034-7>
4. Kazemi Majd F, Fallahi N, Gattulli V (2021) Detection of Corrosion Defects in Steel Bridges by Machine Vision. In International Conference of the European Association on Quality Control of Bridges and Structures August. 2021, pp. 830-834, Springer, Cham
5. Harley J.B, Sparkman D, “Machine learning and NDE: Past, present, and future”, AIP Conference Proceedings 2102, 090001 (2019); <https://doi.org/10.1063/1.5099819>, published Online: 08 May 2019.
6. Obaton A-F, Weaver G, Fournet Fayard L, Montagner F, Burnet O, Van den Bossche A (2022) Classification of metal L-PBF parts manufactured with different process parameters using resonant ultrasound spectroscopy, accepted to *Welding in the World* 10/10/2022
7. ASTM E2001: Guide for resonant ultrasound spectroscopy for defect detection in both metallic and non-metallic parts
8. <https://www.modalshop.com/docs/themodalshoplibraries/white-papers/physical-basis-of-the-resonant-acoustic-method-for-flaw.pdf>
9. Fallahi N, Nardoni G, Heidary H, Palazzetti R, Yan X.T, Zucchelli A (2016) Supervised and non-supervised AE data classification of nanomodified CFRP during DCB tests. *FME Transactions* 44:4: 415-421
10. David A, Vassilvitskii S (2007) K-means++: The Advantages of Careful Seeding. *SODA '07: Proceedings of the Eighteenth Annual ACM-SIAM Symposium on Discrete Algorithms*, 1027–1035
11. Fallahi N (2021) Analysis and optimization of variable angle tow composites through unified formulation. Doctoral dissertation, Politecnico di Torino

12. Forooghi A, Fallahi N, Alibeigloo A, Forooghi H, Rezaey S (2022) Static and thermal instability analysis of embedded functionally graded carbon nanotube-reinforced composite plates based on HSDT via GDQM and validated modeling by neural network. *Mechanics Based Design of Structures and Machines* 1-34. <https://www.tandfonline.com/doi/abs/10.1080/15397734.2022.2094407>
13. A.R. Oskouei, H. Heidary, M. Ahmadi, and M. Farajpur, "Unsupervised acoustic emission data clustering for the analysis of damage mechanisms in glass/polyester composites", *Materials & Design*, 37, 416-422, 2012.
14. Fallahi N, Nardoni G, Heidary H, Palazzetti R, Yan X.T, Zucchelli A (2016) Supervised and Non-supervised AE Data Classification of Nanomodified CFRP During DCB Tests. *FME Transactions* 44:415-421
15. Fallahi N, Nardoni G, Palazzetti R, Zucchelli A (2016) Pattern Recognition of Acoustic Emission signal During the Mode I Fracture Mechanisms in Carbon- Epoxy Composite. 32nd European Conference on Acoustic Emission Testing.
16. Hovde Liland K, Almøy T, Mevik B-H (2010) Optimal Choice of Baseline Correction for ultivariate Calibration of Spectra. *Appl. Spectrosc.* 64:9:1007-1016. <https://doi.org/10.1366/000370210792434350>
17. Meyer D (2022) Support Vector Machines, The Interface to libsvm in package e1071, 1-8. <https://rdr.io/rforge/e1071/f/inst/doc/svmdoc.pdf>
18. Meyer D, Dimitriadou E, Hornik K, Weingessel A, Leisch F, Chang C-C, Lin (2022) Algorithm Library Package 'e1071 52-53. <https://cran.r-project.org/web/packages/e1071/index.html>

Figures

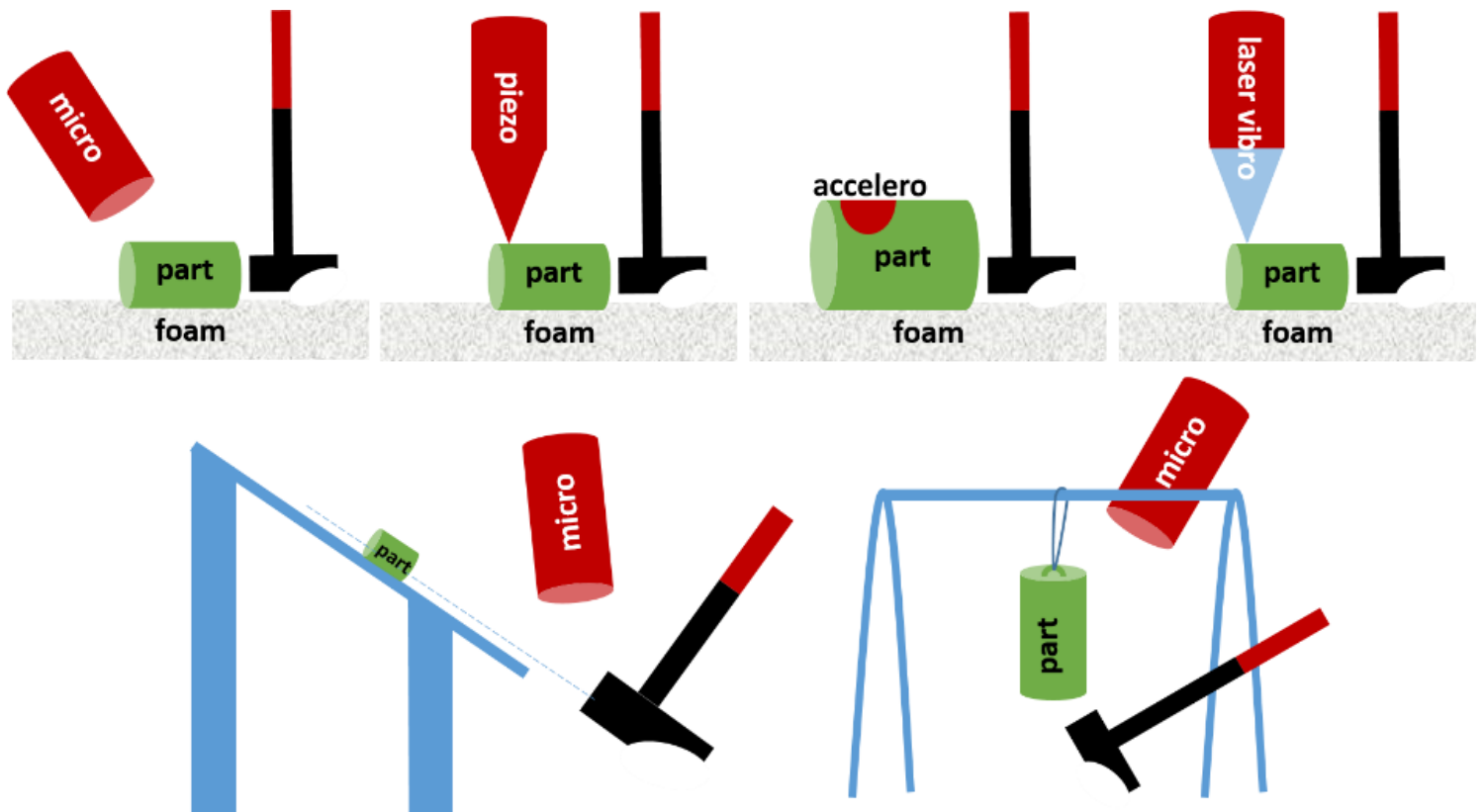


Figure 1

Various schematic representations of the Impulse Excitation Methods (IEM). "micro" stands for microphone, "piezo" for piezoelectric transducer, "accelero" for accelerometer and "laser vibro" for laser vibrometer

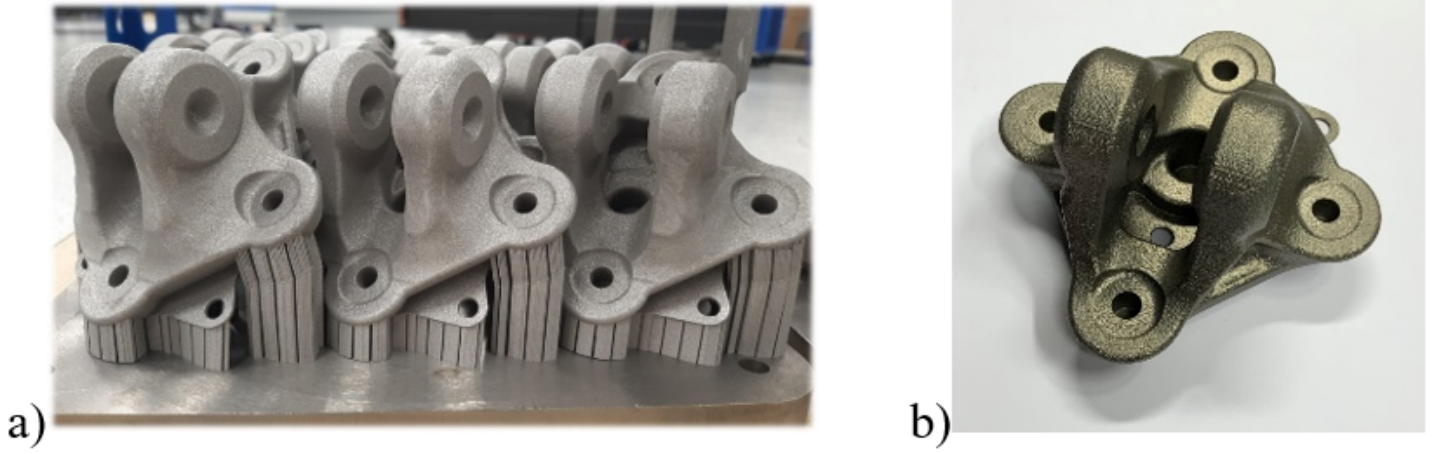


Figure 2

Photographs of the Safran parts on one of the platforms (a) and of an individual part as final (b)

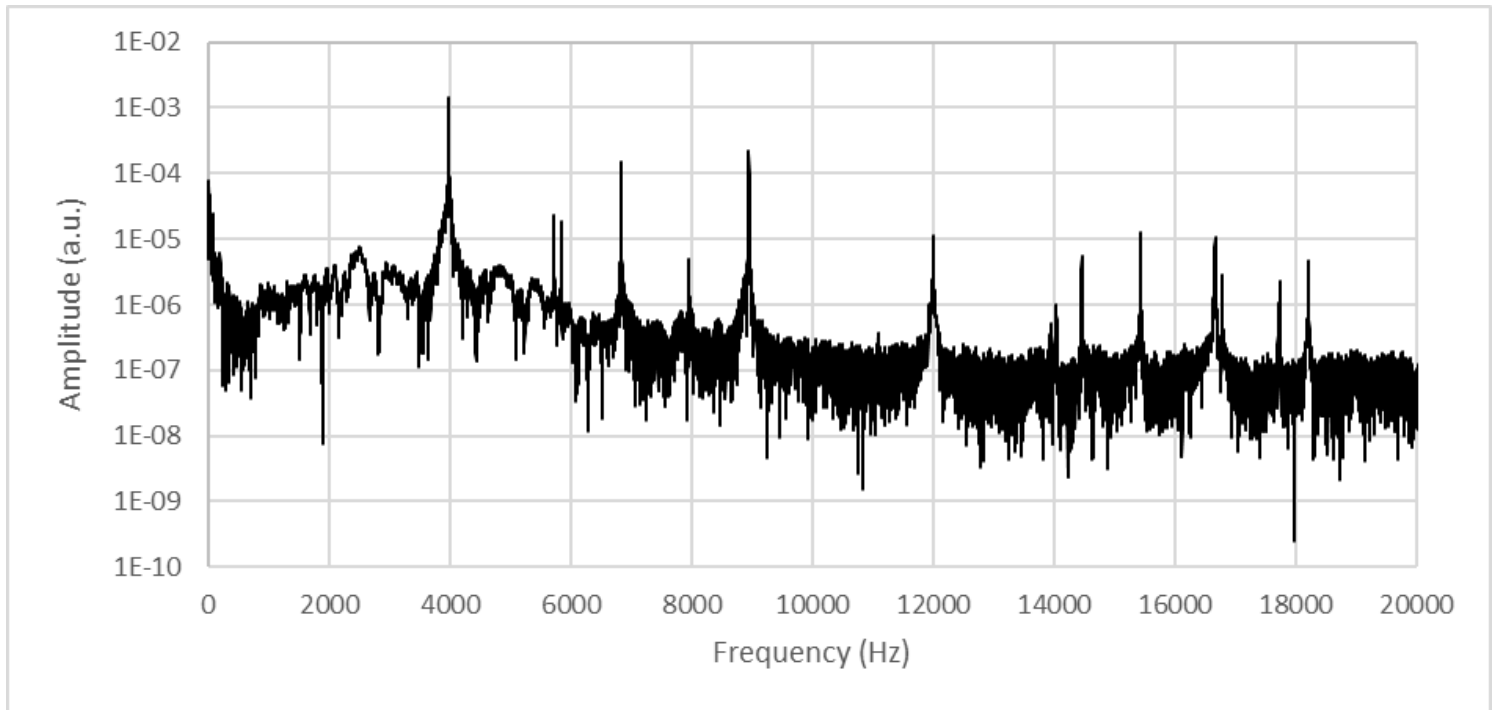


Figure 3

Typical RUS spectrum of the tested part in the range 0-20 kHz corresponding to the first thirteen resonant peaks

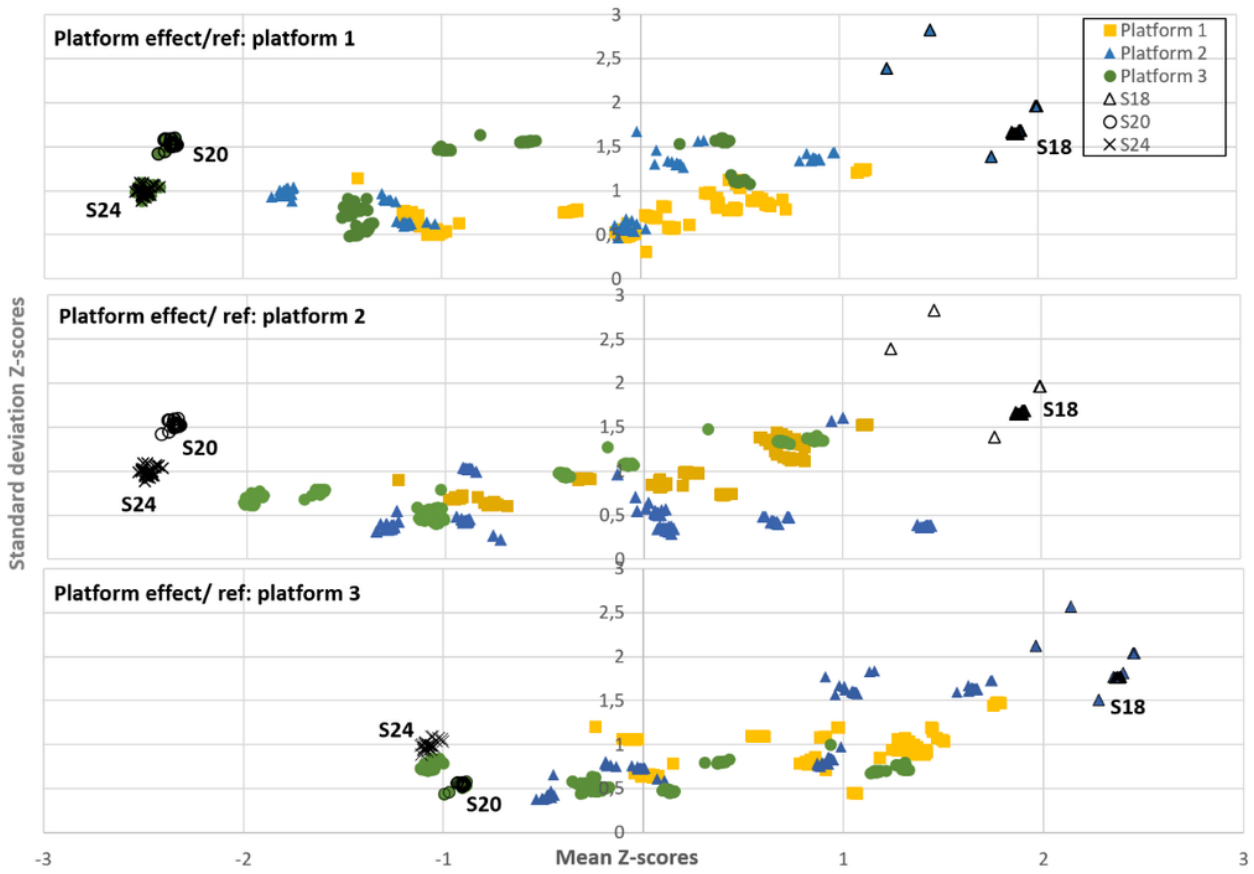


Figure 4

Z-score graphs displaying the platform effect. Each platform was successively considered as reference.

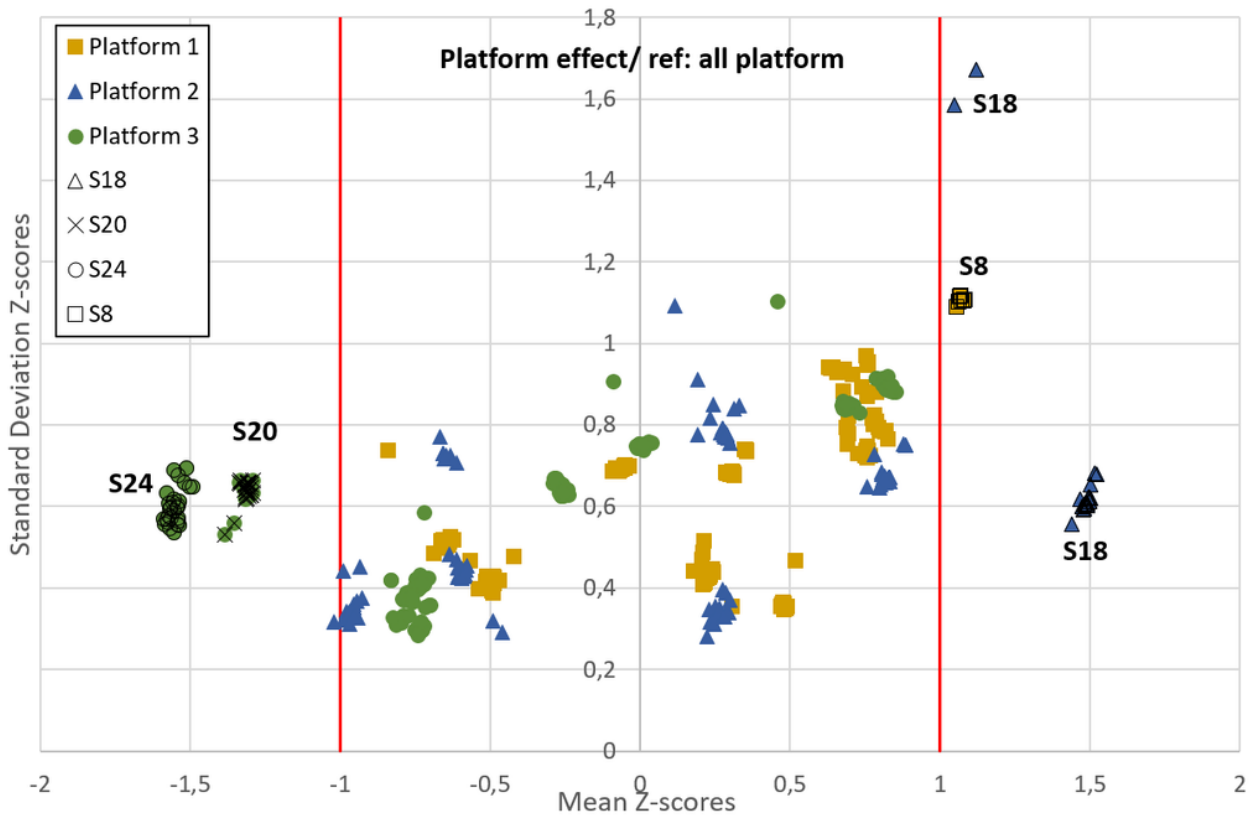


Figure 5

Z-scores' graph to evaluate the platform effect. All platforms were considered as reference

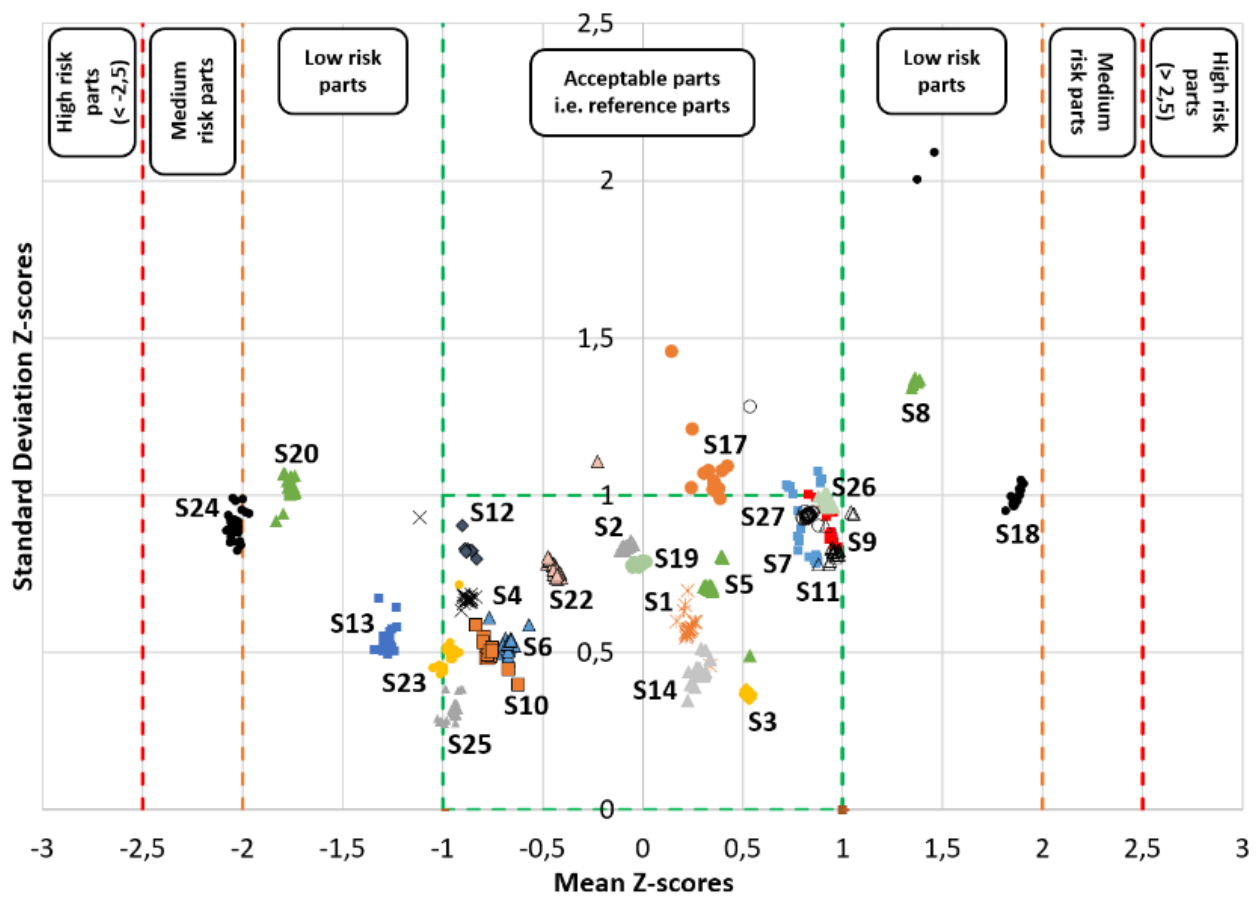


Figure 6

Z-score' graph of the tested parts

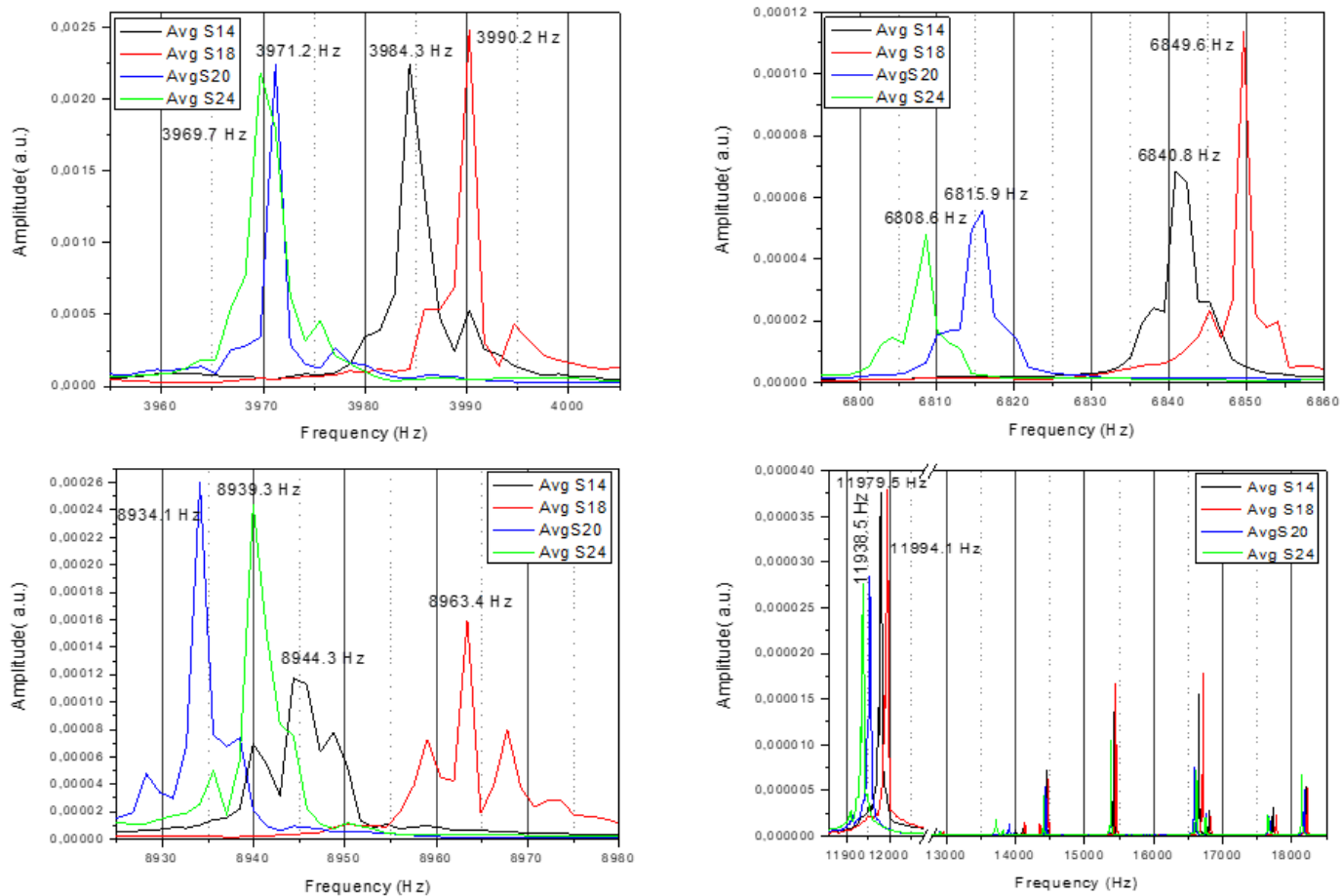
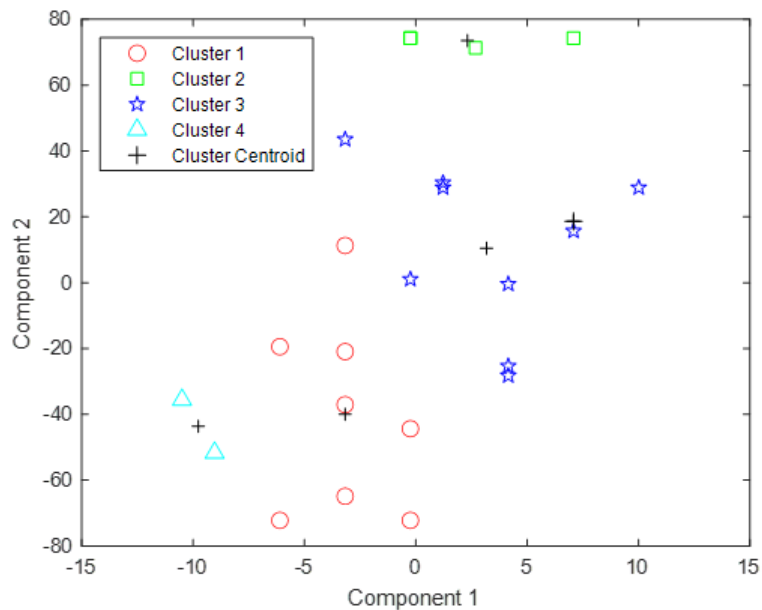


Figure 7

Shifts in frequencies between reference part group S14 and outliers S18, S20 and S24



Cluster number	Part number
Cluster 1	S2, S4, S6, S10, S12, S13, S23, S25
Cluster 2	S5, S8, S19, S27
Cluster 3	S1, S3, S7, S9, S11, S14, S17, S18, S22, S26
Cluster 4	S20, S24

Figure 8

Clustering using K-means with peaks as input. The clusters in 13 dimensions (13 peaks) are represented here in 2 dimensions with the help of principal component analysis. Axis correspond to the 2 directions with maximum standard deviation for better separation of clusters

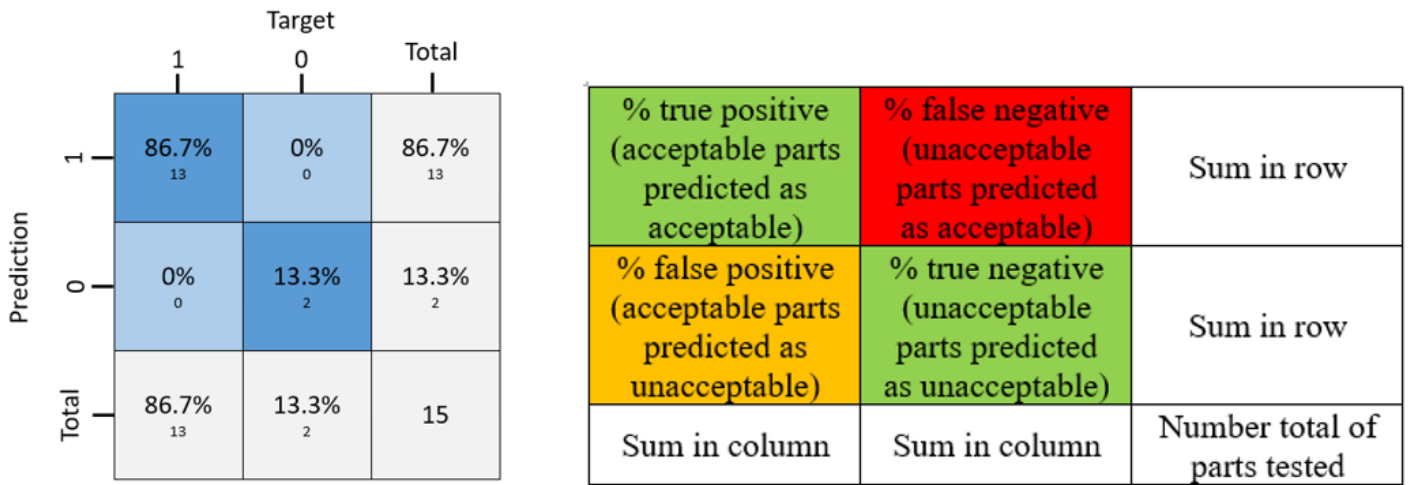


Figure 9

Confusion matrices for Naïve Bayes model, on the test set, with peaks as input. The table located right explained how to understand the confusion matrices. The best is to have maximum percentage in the green boxes, to have a low percentage in the orange box. Having higher than “0” in the red box is problematic. The number “1” indicates that a part is acceptable and “0” that it is not acceptable

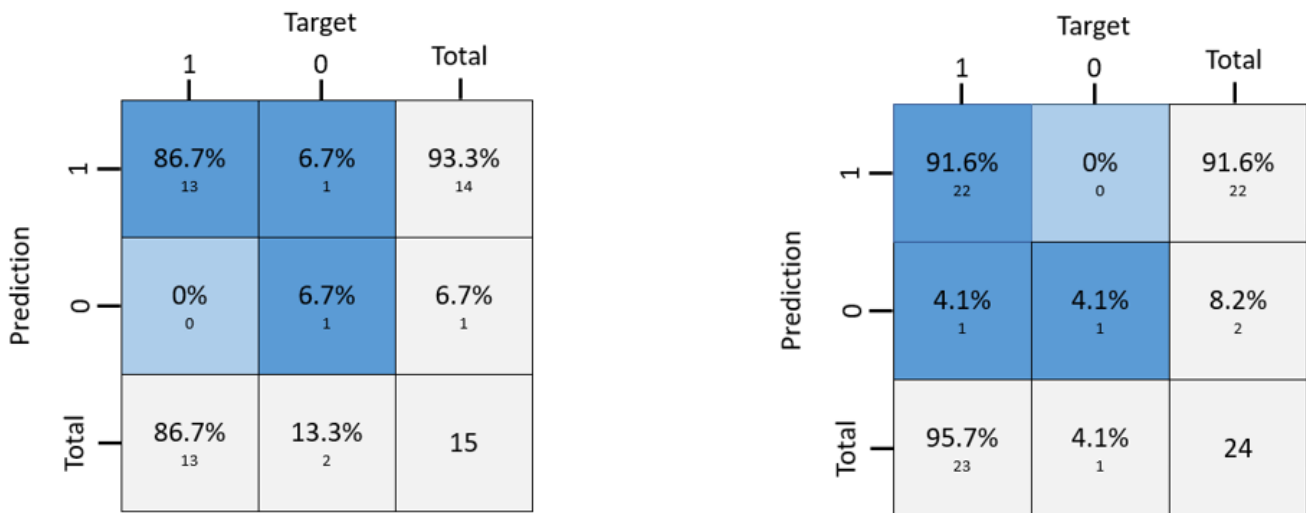


Figure 10

Confusion matrices for Naïve Bayes model with peaks as input. Left: on the test set. Right: on the 24 real parts